Energetics and Volume Changes of the Intermediates in the Photolysis of Octopus Rhodopsin at a Physiological Temperature

Yoshinori Nishioku,* Masashi Nakagawa,† Motoyuki Tsuda,† and Masahide Terazima*
*Department of Chemistry, Graduate School of Science, Kyoto University, Kyoto 606-8502, Japan, and †Department of Life Science, Himeji Institute of Technology, Harima Science Garden City, Kamigori, Akou-gun, Hyogo 678-1297, Japan

ABSTRACT Enthalpy changes (ΔH) of the photointermediates that appear in the photolysis of octopus rhodopsin were measured at physiological temperatures by the laser-induced transient grating method. The enthalpy from the initial state, rhodopsin, to bathorhodopsin, lumirhodopsin, mesorhodopsin, transient acid metarhodopsin, and acid metarhodopsin were 146 ± 15 kJ/mol, 122 ± 17 kJ/mol, 38 ± 8 kJ/mol, 12 ± 5 kJ/mol, and 12 ± 5 kJ/mol, respectively. These values, except for lumirhodopsin, are similar to those obtained for the cryogenically trapped intermediate species by direct calorimetric measurements. However, the ΔH of lumirhodopsin at physiological temperatures is quite different from that at low temperature. The reaction volume changes of these processes were determined by the pulsed laser-induced photoacoustic method along with the above ΔH values. Initially, in the transformation between rhodopsin and bathorhodopsin, a large volume expansion of +32 ± 3 ml/mol was obtained. The volume changes of the subsequent reaction steps were rather small. These results are compared with the structural changes of the chromophore, peptide backbone, and water molecules within the membrane helixes reported previously.

INTRODUCTION

The enthalpy change (ΔH) and the volume change (ΔV) of a biochemical reaction traditionally have been measured by a calorimetric method for one-step reactions or from the temperature or pressure dependence of the equilibrium constants for reversible reactions (Lamola et al., 1974; Tsuda and Ebrey, 1980). A unique way to measure the ΔH of an unstable intermediate species, in particular for a biological macromolecule, is the direct calorimetric technique by trapping the unstable species at a low temperature. Cooper and coworkers utilized this technique to measure the enthalpy changes associated with the kinetic steps in the bleaching of bovine rhodopsin (Cooper, 1979, 1981) and octopus rhodopsin (Cooper et al., 1986). These data have frequently been used for analyzing or interpreting biochemical reactions (Bagley et al., 1989; Deng et al., 1991a,b). However, there is no guarantee that the enthalpy changes of a cryogenically trapped species are same as that of the intermediate species at physiological temperatures, because structural changes of the chromophore, peptide backbone, and water molecules could be suppressed at low temperature; in addition, these enthalpy values could be temperature dependent. Despite these concerns, it has been impossible to study the enthalpy changes at physiological temperatures because the traditional method cannot be used to study irreversible reactions of multi-step processes. In this paper, we report ΔH and ΔV of the intermediate species in the photolysis of octopus rhodopsin (Rh) at physiological temperatures using the time-resolved transient grating (TG) and pulsed laser-induced photoacoustic (PA) methods.

Octopus rhodopsin is present in the microvillar membranes of the photoreceptor cells (Tsuda, 1987). Its chromophore is 11-*cis* retinal bound to the lysine residue via a protonated Schiff base. After photoisomerization of the 11-*cis* chromophore to the all-*trans* form, a series of thermal reactions takes place. These photointermediates have been identified by transient absorption spectroscopy, and they are consecutively called primerhodopsin (Prime), bathorhodopsin (Batho), lumirhodopsin (Lumi), mesorhodopsin (Meso), and acid metarhodopsin (Acid Meta) (Tsuda, 1979; Ohtani et al., 1988; Taiji et al., 1992; Nakagawa et al., 1997). The structural changes of the chromophore, peptide backbone, and water of these intermediates have been studied by resonance Raman (Kitagawa and Tsuda, 1980; Pande et al., 1987; Deng et al., 1991a,b; Huang et al., 1996, 1997; Hashimoto et al., 1996), FTIR (Masuda et al., 1993a,b; Bagley et al., 1989; Nishimura et al., 1997), and UV difference absorption spectroscopy (Nakagawa et al., 1997). Recently, we showed that regions of the protein distant from the chromophore are still changing even after the changes in the microenvironment around the chromophore are over. We referred to the intermediate that is produced accompanying the final chromophore absorption change as transient acid metarhodopsin (Transient Acid Meta) (Tsuda, 1979; Masuda et al., 1993); it has a different protein conformation from the stable final photoproduct, acid metarhodopsin (Nishioku et al., 2001). This is consistent with our previous report that the stable final photoproduct could not activate the G-protein, and hence a transient intermediate which lies between Meso and stable Acid Meta must be the activating species (Nakagawa et al., 1998). Thus, we hypothesize that the Transient Acid Meta activates the G-protein and is transformed isospectrally to stable Acid Meta (Fig. 1).

Submitted January 16, 2002, and accepted for publication March 27, 2002.
Address reprint requests to Dr. Masahide Terazima, Department of Chemistry, Graduate School of Science, Kyoto University, Kyoto 606-8502, Japan. Tel.: 81-75-753-4026; Fax: 81-75-753-4000; E-mail: mterazima@kuchem.kyoto-u.ac.jp.

0006-3495/02/08/1136/11 $2.00

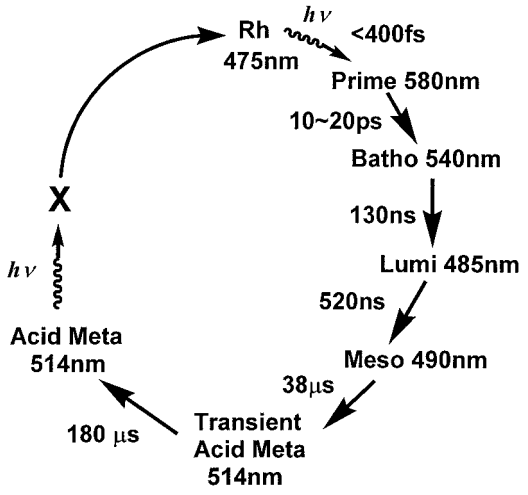

FIGURE 1 Schematic illustration of the photoreactions of octopus rhodopsin. (Rh is rhodopsin, Prime is primerhodopsin, Batho is bathorhodopsin, Lumi is lumirhodopsin, Meso is mesorhodopsin, Transient Acid Meta is transient acid metarhodopsin, and Acid Meta is acid metarhodopsin; X is an intermediate that was produced upon photolysis of Acid Meta.) The wavelengths at the absorption maxima and the lifetimes of the intermediates at 15°C are also shown.

The PA method can uniquely measure the volume change and the enthalpy change of irreversible chemical reactions (Braslavsky and Heibel, 1992; van Brederode et al., 1995). Indeed, this method has been applied to the photoreactions of bacteriorhodopsin (Schulenberg et al., 1994; Zhang and Mauzerall, 1996), bovine rhodopsin (Strassburger et al., 1997; Gensch et al., 1998), and sensory rhodopsin I (Losi et al., 1999). However, the time window of the PA signal is not wide enough (usually 10 ns to ~10 μs) to measure the whole process of the photolysis of visual pigments. The sensitivity within this time window is not uniform, and the dynamics near the limit of the window are insensitive. Thus we used the TG and transient lens (TrL) method to measure the energy levels of the irreversible reactions over a wide time scale (Terazima, 1998). After we determined the thermal energy from each process using the TG and TrL method, the reaction volume of these processes was extracted using the PA measurements. Using this strategy, we determined the enthalpy and volume change of each intermediate in the photolysis of octopus rhodopsin at physiological temperatures. Although most of the ΔH values are similar to those measured for the cryogenically trapped species, the ΔH in forming Lumi is quite different. These ΔH values are discussed in the context of previous findings on the pigment's conformational changes.

MATERIALS AND METHODS

Octopus rhodopsin was prepared as described previously (Tsuda et al., 1986). Briefly, microvillar membranes from octopus retinas (*Octopus dofleini*) were isolated by sucrose flotation, and the membranes were solubilized in 1% (w/v) sucrose monolaurate (SM 1200), 10 mM Tris-HCl buffer (pH 7.4) containing 1 mM dithiothreitol, 1 mM benzamidine-HCl, and 20 μM 4-(amidinophenyl)methanesultonylfluoride hydrochloride (APMSF). Octopus rhodopsin was affinity purified by concanavalin-A Sepharose (Amersham Pharmacia Biotech, Uppsala, Sweden). The sample (~80 μM rhodopsin) for the transient grating and photoacoustic measurements was prepared in 10 mM MOPS (pH 7.4) and 1% sucrose monolaurate.

The TG setup was similar to that described previously (Terazima and Hirota, 1993; Hara et al., 1996; Nishioku et al., 2001). Briefly, the beam of a XeCl excimer laser-pumped dye laser (Lamda Physik Compex 102xc, Göttingen, Germany, Lumomics Hyper Dye 300; λ = 465 nm) was divided by a beam splitter and the beams crossed inside a quartz sample cell (optical path-length = 2 mm). The laser power of the excitation was <5 μJ/pulse. The interference pattern (transient grating) created in the sample was probed by a diode laser (840 nm) as a Bragg diffracted signal (TG signal). The grating wavenumber, q, was varied by changing the crossing angle of the excitation and probe beams.

The experimental setup for the TrL method has also been described in detail (Terazima and Hirota, 1993). In the TrL method, the excitation beam was focused in the sample solution. A He-Ne laser beam (633 nm) was collinearly brought into the sample cell, and the intensity of the beam center at a far point was monitored by a photomultiplier through a pinhole and a glass filter. The TG signals and TrL signals were detected by a photomultiplier (Hamamatsu R928, Iwata, Japan) and averaged by a digital oscilloscope (Tektronix 2430A, Tokyo, Japan).

The PA signal was detected by a piezoelectric transducer (PZT and PCB 132A32, Tokin, Sendai, Japan) as described previously (Terazima and Azumi, 1989). The signal was directly detected by a digital oscilloscope and averaged.

We were extremely careful for the data acquisition condition. The repetition rate of the excitation laser was <1 Hz. After every two laser shots, the sample solution was stirred to prevent the accumulation of photoproducts in the excitation region. At the same time, between every measurement, the sample was irradiated with orange light (a tungsten lamp with a cutoff filter (λ > 590 nm)) to convert the Acid Meta photoproduct back to rhodopsin (Tsuda, 1979, 1987). The orange light was blocked during the measurement. The excitation beam was focused to the sample with a 1-mm diameter. The light irradiated volume was ~1.5×10^{-3} ml. This photo-irradiated volume is negligibly small compared with the total sample volume, 0.6 ml. Therefore, the photoexcitation of the photoproduct should be neglected for the measurement under this condition. Furthermore, we used a laser power of typically 1 μJ/pulse for quantitative ΔH and ΔV measurements. Under this condition, the concentration of photoexcited molecule was ~2.5 μM, which was much smaller than a typical sample concentration of 80 μM. Therefore, the effect of the photobleaching could be completely neglected. We confirmed that the refractive index change (square root of the TG signal and signal intensity of the TrL signal) was proportional to the laser power.

Experiments were performed over an −0.5~35°C range with a temperature-controlled thermal bath (Lauda RSD6D). Bromocresol purple (BCP) was used for a calorimetric reference. Because the lifetimes of the excited states of BCP are less than 1 ns and the radiative transitions as well as photochemical reaction are negligible, all of the absorbed photon energy should be released within the pulse width of our excitation laser. The absorbance of BCP was adjusted to the same value as that of the octopus rhodopsin sample at the excitation wavelength. The value of q was determined from the decay rate of the thermal grating signal of this reference sample (vide infra).

Principles

TG method

In the TG method, a sinusoidal modulation of the light intensity is produced by the interference of two light waves. Photoexcitation of the sample

by this light creates a sinusoidal modulation in the refractive index and in the absorbance caused by the factors discussed below. Under weak diffraction conditions, the TG signal intensity (I_{TG}) is proportional to the square of the variations in the refractive index (δn) and in the absorbance (δk).

The refractive index change consists of the following three components: contributions of released heat (δn_{th}, thermal grating), the molecular refractive index difference between the reactant and products due to the change of the absorption spectrum (δn_{pop}, population grating), and the density change caused by the reaction volume (δn_v, volume grating). We call the sum of δn_{pop} and δn_v the species grating (δn_{spe}), because the time profiles of δn_{pop} and δn_v are identical for most cases. The TG signal intensity (I_{TG}) is given by

$$I_{TG}(t) = \alpha(\delta n_{th}(t) + \delta n_{pop}(t) + \delta n_v(t))^2, \quad (1)$$

where α is a constant representing the sensitivity of the system.

The temporal evolution of $\delta n_{th}(t)$ reflects the time dependence of the thermal energy being released. Solving the thermal diffusion equation, one obtains (Terazima, 1998)

$$\delta n_{th}(t) = \left(\frac{dn}{dT}\right)\frac{W}{\rho C_p}[dQ(t)/dt * \exp(-D_{th}q^2t)], \quad (2)$$

where * represents the convolution integral, $Q(t)$ is the thermal energy coming out from the photoexcited rhodopsin, W is molecular weight, dn/dT is the temperature dependence of the refractive index, ρ is the density, C_p is the heat capacity at constant pressure, and D_{th} is the thermal diffusivity. The grating wavenumber, q, is given by $q = \pi \sin(\theta/2)/\lambda_{ex}$ (λ_{ex} is wavelength of the excitation light). We can vary q by varying the crossing angle (θ) between two excitation beams. The proportionally constant α in Eq. 1 can be determined by comparison of the signal intensity with that of the calorimetric reference sample, which releases the absorbed photon's energy as thermal energy within our time resolution. By analyzing the time profile of the thermal grating signal with Eq. 2, the thermal energy associated with each reaction process can be measured and the enthalpy of each species can be calculated. In this paper, the enthalpy of each species (ΔH) is defined by the enthalpy difference from that of the original species, Rh.

$$Q(t) = \Delta N(h\nu - \Phi\Delta H), \quad (3)$$

where Φ is the quantum yield of the reaction, ΔN is the number of the reacting molecules in a unit volume and $h\nu$ is the photon energy for the excitation. The refractive index change after photoexcitation of a calorimetric reference sample, which converts all of the excitation photon energy to the thermal energy faster than the time-response (δn_{th}(reference)) is given by

$$\delta n_{th}(\text{reference}) = \left\{\left(\frac{dn}{dT}\right)\frac{\Delta N h\nu W}{\rho C_p}\right\}\exp(-D_{th}q^2t) \quad (4)$$

By taking a ratio of δn_{th} of the sample (δn_{th}(sample)) to δn_{th}(reference), ΔH can be calculated by

$$\frac{\delta n(\text{sample})}{\delta n(\text{reference})} = 1 - \frac{\Phi\Delta H}{h\nu} \quad (5)$$

The refractive index change due to the volume grating is given by

$$\delta n_v = V\frac{dn}{dV}\Delta V\Delta N, \quad (6)$$

where Vdn/dV is the refractive index change by the molecular volume change. By taking a ratio of δn_v to δn_{th}(reference) with the known solvent property (Vdn/dV), ΔV can be determined.

The time dependence of the species grating is determined by the kinetics of the reaction and the molecular diffusion process. If we can neglect the reaction kinetics in the molecular diffusion time region, the time dependence is given by (Terazima and Hirota, 1993; Hara et al., 1996)

$$\delta n_{spe}(t) = -\delta n_r \exp(-D_r q^2 t) + \delta n_p \exp(-D_p q^2 t), \quad (7)$$

where q is a grating wavenumber, and δn_r and δn_p represent refractive index changes by the reactant and product, respectively. D_r and D_p are the molecular diffusion coefficients of the reactant and product, respectively. The reaction kinetics can be separated from the diffusion process by measuring the transient grating dynamics at different q^2, because the diffusion process depends on q^2, whereas the reaction kinetics should not.

TrL method

In the TrL method, a sample is excited with a pump beam having a spatially Gaussian form, so that the profile of the concentration of the excited-state molecules should be the same Gaussian. If the refractive index or the absorption changes by any of the reasons described above, the spatial profile of this change should also be a Gaussian. At the central part, the Gaussian profile of the refractive index acts as a lens to expand (or focus) another light beam passing through that region. The expansion (or focusing) of the light beam can be detected as a change in the light density through a pinhole placed at a far field.

The TrL signal intensity (I_{TrL}) is proportional to the refractive index change induced by the photoexcitation.

$$I_{TrL}(t) = \alpha'(\delta n_{th-L}(t) + \delta n_{spe-L}(t) + \delta k_{spe-L}(t)), \quad (8)$$

where α' is the proportional constant, and $\delta n_{th\text{-}L}(t)$ and $\delta n_{spe\text{-}L}(t)$ are the refractive index change caused by the thermal lens and species lens effect, respectively. The $\delta n_{spe\text{-}L}(t)$ includes the volume lens and population lens effects same as the species grating. Because the TrL signal reflects the refractive index change due to photoexcitation, the information from the signal is essentially identical to that obtained from the TG method. One notable difference is the decay rate constant of the signal. Whereas the decay rate of the thermal grating signal is ~1–10 μs usually, that of the thermal lens signal is ~10 ms, which is determined by the thermal diffusion time across the focused beam diameter (~100 μm). Here, this slower time constant is an advantage for measuring the enthalpy of a slowly created species.

PA method

In PA detection, the pressure wave is detected by a pressure-sensitive device such as a piezoelectric transducer. The magnitude of the pressure wave is proportional to the density change of the matrix through the thermal effect and volume effect. The time profile of the PA signal of the sample (rhodopsin) by the PA method, $S(t)$, is given by a convolution between the PA signal of the calorimetric reference $g(t)$ and a time dependent pressure evolution $P(t)$ (Terazima and Azumi, 1989; van Brederode et al., 1995; Strassburger et al., 1997):

$$S(t) = P(t) * g(t) \quad (9)$$

RESULTS

Time profile of the TG signals of octopus rhodopsin

Fig. 2, *A—C*, shows the time profiles of the TG signals of the octopus rhodopsin (~80 μM) upon photoexcitation (465 nm) probed at 840 nm at 20°C with $q^2 = 2.0 \times 10^{12}$ m^{-2}.

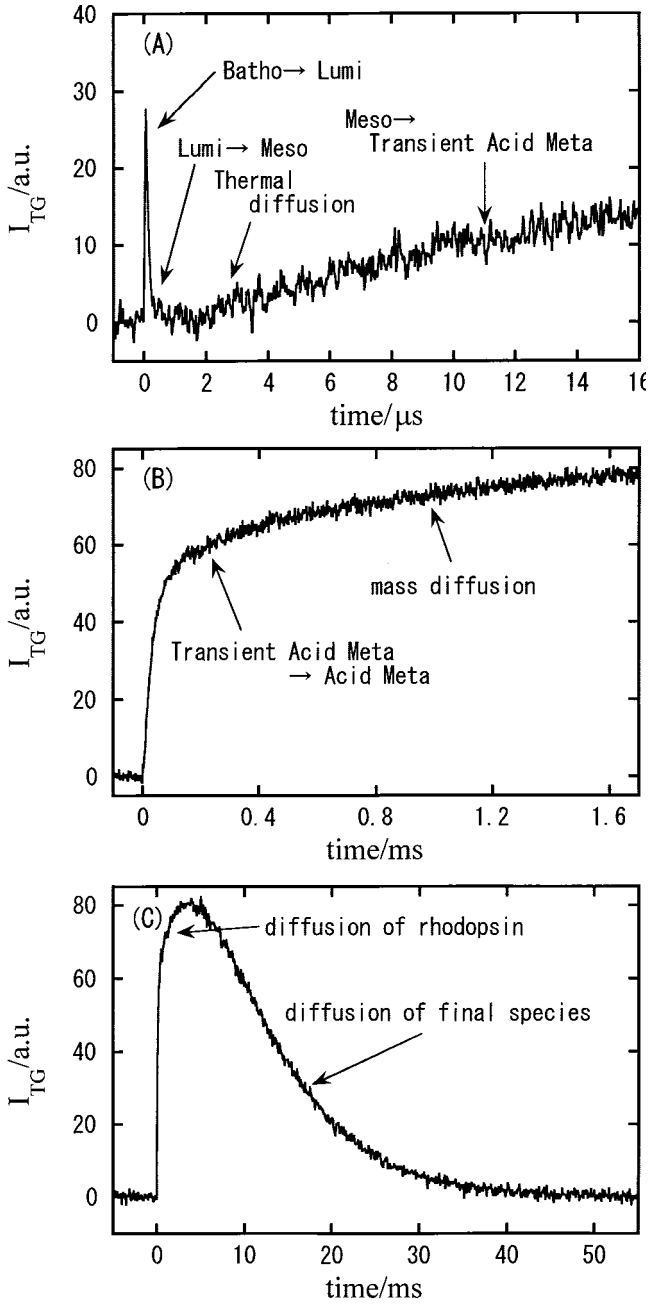

FIGURE 2 The kinetics of the TG signal of octopus rhodopsin after 465-nm pulse probed at 840 nm at 20°C on three different time scales at $q^2 = 2.0 \times 10^{12}$ m^{-2}. The sample concentration is 80 μM. (*A*) The fast time scale (<20 μs); (*B*) the middle time scale (<2 ms); (*C*) The slower time scale (>2ms). The assignments of the kinetic components are labeled in the figure.

The qualitative features of the observed TG signal were described in an earlier paper (Nishioku et al., 2001). Briefly, the signal rises within 10 ns after the photoexcitation followed by a decay with a tri-exponential function and a single-exponential rise within a time window of 10 ns to ~20 μs (Fig. 2 *A*). One of the rate constants depends on q^2, but the other does not. The q^2-dependent kinetics is attributed to the thermal grating signal and the q^2-independent kinetics represents the transformation of the Batho to Meso form. The main part of this q^2-independent signal originates from the change of the absorption spectra of Rh (the population grating component). Considering previous studies on the photoreactions of Rh using the transient absorption method, we can attribute these dynamics to the reactions of Batho → Lumi → Meso → Transient Acid Meta. The rate constants of the TG signal agree quite well with those determined by the transient absorption method.

After the transformation of Meso to Transient Acid Meta with a lifetime of 23 μs at 20°C, the TG signal rises with a bi-exponential function on a much longer time scale (Fig. 2 *B*) and finally decays to the baseline as a single exponential (Fig. 2 *C*). The first rise rate does not depend on q^2 (180 μs at 15°C and 150 μs at 20°C); hence it represents the intrinsic kinetics of the protein conformational changes. However, there is no kinetics observed by transient absorption measurements corresponding to this rate. Hence this TG-observed signal is an optically silent transition, and the origin of this signal has previously been attributed to the volume grating component, which comes from the protein structural changes that do not affect the chromophore (Nishioku et al., 2001). At the grating wavenumber we usually used ($q^2 = 0.9$ to 4.0×10^{12} m^{-2}), we observed rise-decay dynamics after this signal and found that this rate constant depends on q^2. Therefore, these decay rates should represent molecular diffusion processes of the species that exist at this time.

In our earlier paper (Nishioku et al., 2001), we described the observation of the 180-μs component and attributed it to the decay of Transient Acid Meta. However, at that time, we could not identify the precursor species; the 180-μs dynamics could correspond to Transient Acid Meta → Acid Meta or it could represent the creation of another intermediate before the final Acid Meta. If we could monitor the TG signal over a much longer time scale, we might be able to distinguish these two possibilities. It was impossible at the previous grating wavenumber, because the signal due to molecular diffusion (vide infra) rises after the 180-μs signal and masks the TG signal at longer times. Here, to remove the diffusion kinetics from the observation time window, we tried to measure the TG signal under a much lower q condition. We successfully observed the TG signal at $q^2 = 2.6 \times 10^{10}$ m^{-2} by careful elimination of the scattered light from the probe beam. At this q^2, we could observe the TG signal until 35 ms without disturbance by the diffusion signal. However, we could not observe any q-independent dynamics after the 180-μs dynamics. Therefore it is highly plausible that the 180-μs dynamics at 20°C represents the Transient Acid Meta → Acid Meta process (Fig. 1).

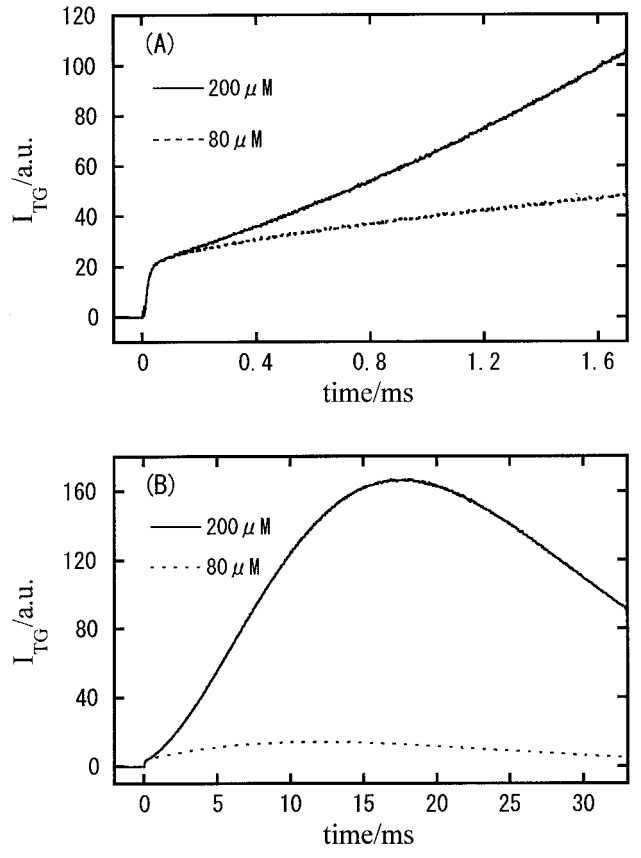

FIGURE 3 The comparison between the TG signal of octopus rhodopsin after 465-nm excitation pulse probed at 840 nm at 200 μM (——) and 80 μM (· · ·) at $q^2 = 1.1 \times 10^{12}$ m^{-2}. (*A*) The middle time scale (<2 ms); (*B*) The slower time scale (>2 ms).

In summary, the time profile of the TG signal over this wide time range (10 ns to 100 ms) can be expressed by

$$I_{TG}(t) = [\mathrm{A}\exp(-k_1 t) + \mathrm{B}\exp(-k_2 t) + \mathrm{C}\exp(-D_{th}q^2 t) + \mathrm{D}\exp(-k_3 t) + \mathrm{E}\exp(-k_4 t) + \mathrm{F}\exp(-D_5 q^2 t) + \mathrm{G}\exp(-D_6 q^2 t)]^2, \quad (10)$$

where A–G are pre-exponential factors of these exponential terms, $k_1 > k_2 > k_3 > k_4$ and $D_5 > D_6$. As described above, k_1 to k_4 correspond to the rate constants of the Batho → Lumi → Meso→ Transient Acid Meta→ Acid Meta processes, respectively. From the measurements at various q^2, D_5 and D_6 are determined to be 0.93×10^{-10} m^2/s and 0.27×10^{-10} m^2/s. These values were used for the fitting of the TG signal. However, further discussion concerning these diffusion coefficients is not within the scope of this paper and will be published later.

This temporal profile does not change by diluting the sample concentration further (<100 μM). However, when the concentration of the sample is increased (>100 μM), the last part of the signal (Fig. 2 *C*) becomes very intense and the time profile becomes different from that at lower concentrations (Fig. 3). This concentration-dependent change can be explained by the formation of aggregates of the molecules. We performed the TG experiment using a diluted solution (<100 μM) for the following quantitative measurements of ΔH and ΔV.

Enthalpy changes of intermediate species at physiological temperatures

The origin of the thermal grating signal is the thermal energy due to the nonradiative transition and the enthalpy changes accompanying the photolysis of octopus rhodopsin. Therefore, if we can measure the time profile of the thermal grating signal of the photochemical sequence of octopus rhodopsin, we can determine the enthalpies of these intermediates step by step from the intensities of the signals. Because a typical decay rate of the thermal grating component under the present experimental condition is 2–6 μs, the thermal energies that come out from the processes of the Rh* (photoexcited state of rhodopsin) → Batho → Lumi → Meso are accumulated to give rise to the rising components of the thermal grating signal. On the other hand, because the rate of the thermal energy release from the process of the Meso → Transient Acid Meta is slower than the thermal diffusion process, the thermal grating intensity due to this process becomes very weak. First, we determine the enthalpies of Batho, Lumi, and Meso by the TG method.

Because the kinetics from Rh* to Batho are faster than our time resolution, the thermal energy we can observe here is expressed by

$$Q(t) = Q_f(t) + Q_{s1}[1 - \exp(-k_{s1}t)] + Q_{s2}[1 - \exp(-k_{s2}t)], \quad (11)$$

where Q_f denotes the fast thermal energy (within the pulse width), and $Q_{s1}$and Q_{s2} are the thermal energies accompanied with transitions of the Batho → Lumi and Lumi → Meso. A difficulty we encounter for the quantitative measurement of the thermal grating signal comes from interference by the species grating signal of the transition of the Batho to Transient Acid Meta. We estimated the species grating signal contribution by measuring the TG signal at two temperatures as follows.

It is well known that dn/dT in Eq. 2 of an aqueous solution is strongly dependent on temperature, and it almost vanishes at ~0°C. Because δn_{th} is proportional to dn/dT, the TG signal at this temperature should represent the species grating signal. First, to examine the temperature dependence of dn/dT of the buffer solution we used, we measured the TG signal of the calorimetric standard sample in the buffer at various temperatures. We found that the thermal grating signal that is proportional to dn/dT almost vanishes at −0.5°C. Therefore, the grating signal at this temperature (Fig. 4) should be free from the thermal contribution and

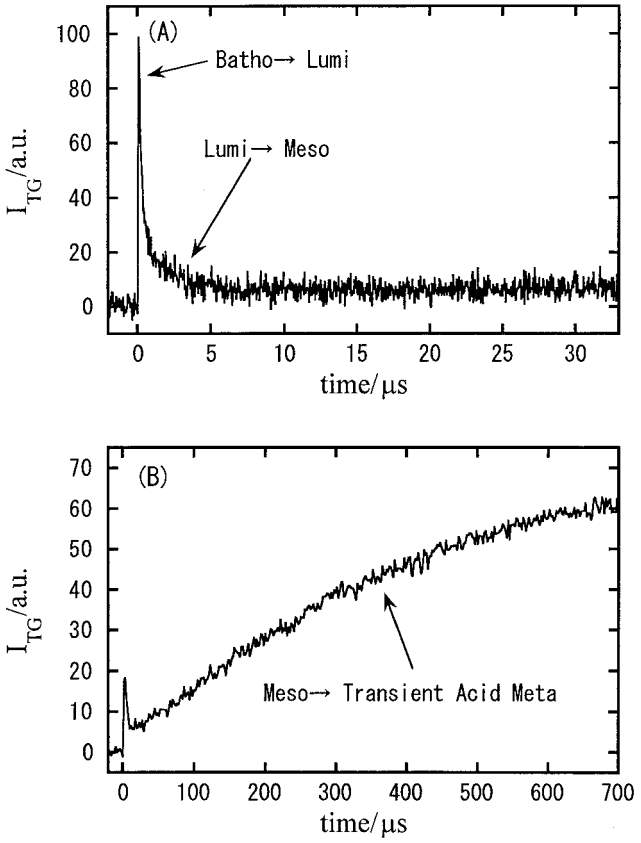

FIGURE 4 The time profile of the TG signal of octopus rhodopsin after 465-nm excitation pulse probed at 840 nm at −0.5°C. The sample concentration is 80 μM. Assignment of each kinetics is labeled in the figure. Because *dn/dT* is zero in this solution at −0.5°C, the TG signal in this figure represents only species grating signal.

consists of only the species grating contribution. The signal at −0.5°C ($\delta n_{spe}(t, T = -0.5°C)$) was fitted by a sum of three exponential functions corresponding to the Batho → Lumi → Meso → Transient Acid Meta processes as

$$\delta n_{spe}(t, T = -0.5°C) = \delta n^0_{spe}\{1 + 0.73 \exp(-t/270\ \text{ns}) + 0.41 \exp(-t/2.5\ \mu\text{s}) - 0.55 \exp(-t/239\ \mu\text{s}) \quad (12)$$

Next, we estimated the species grating signal at 20°C to determine the thermal grating signal contribution. For estimating the species grating signal at 20°C from that at $T = -0.5°C$, we examined the transient absorption signal at various temperatures and found that the signal at 20°C can be fitted by the sum of exponential functions with the same amplitude at −0.5°C. This fact implies that quantum yield of the reaction as well as the production yields of the intermediate species (pre-exponential factor of δn_{spe}) do not depend on the temperature. Hence, the species grating signal at 20°C can be constructed by using the same pre-exponential factors of Eq. 12 with the rate constants determined by the transient absorption and the TG signals at 20°C:

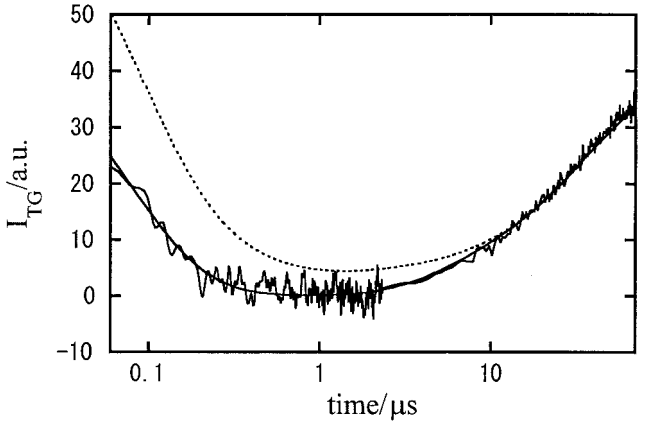

FIGURE 5 The time profile of the TG signal of octopus rhodopsin after 465-nm excitation pulse probed at 840 nm at 20°C (——) and the calculated curve of the species grating signal at 20°C (· · ·). The difference between these two curves represents the contribution of the thermal grating. The smooth solid line expresses the fitting curve with a superposition of the calculated species grating signal and the thermal grating contribution.

$$\delta n_{spe}(t, T = 20°C) = \delta n^0_{spe}\{1 + 0.73 \exp(-t/113\ \text{ns}) + 0.41 \exp(-t/360\ \text{ns}) - 0.55 \exp(-t/23.4\ \mu\text{s}) \quad (13)$$

Thus calculated species grating and the observed TG signals are depicted in Fig. 5. The difference between the calculated and the observed signals should represent the contribution of the thermal grating contribution. We fitted the observed TG signal at 20°C by the least-square fitting with Eq. 13, adding

$$\delta n_{th}(t) = \delta n_{th,f} + \delta n_{th,s1}[1 - \exp(-t/113\ \text{ns})] + \delta n_{th,s2}[1 - \exp(-t/360\ \text{ns})] \quad (14)$$

The pre-exponential factor of Eq. 14 represents the released energy by these processes (Eqs. 2 and 11). As mentioned in Principles, comparing the thermal grating signal intensity of the sample with that of the reference, we can determine the enthalpy change from Eq. 5. From the experimentally determined ratio δn_{th}(Rh*-Batho)/δ n_{th}(reference) = 0.72, δn_{th}(Rh*-Lumi)/δ n_{th}(reference) = 0.76, δn_{th}(Rh*-Meso)/δ n_{th}(reference) = 0.93 and $\Phi = 0.5$ (Ohtani et al., 1988), we obtained $\Delta H_{Batho} = 146 \pm 15$ kJ/mol, $\Delta H_{Lumi} = 122 \pm 17$ kJ/mol and $\Delta H_{Meso} = 38 \pm 8$ kJ/mol. Almost the same values can be also obtained at 25°C. The photon energy we used is 257 kJ/mol. Hence, most of the absorbed energy is released as heat within 500 ns at 20°C.

Next, the enthalpy of Transient Acid Meta was determined by using the TrL method. As stated above, because

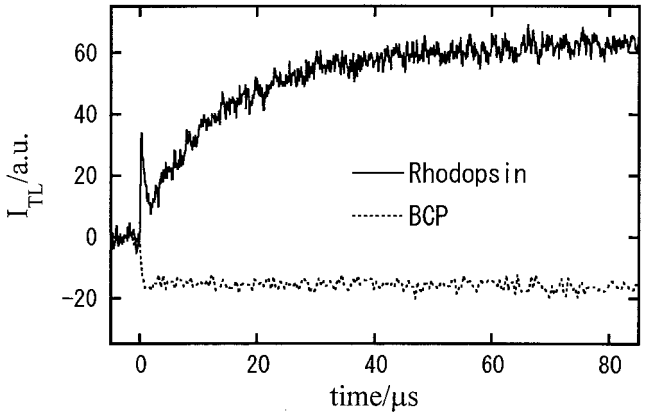

FIGURE 6 The time profiles of the TrL signals of octopus rhodopsin (——) and BCP reference (dotted line) after 465 nm excitation pulse probed at 633 nm at 24°C. Absorbance at 465 nm of octopus rhodopsin sample and BCP reference are same (Absorbance = 0.45, path-length = 2 mm).

the lifetime of the Meso → Transient Acid Meta process is longer than the decay rate of the thermal grating, the signal intensity becomes very weak, and it was impossible to measure this quantity by the TG method. However, the decay rate of the thermal lens signal is much slower than the thermal grating, and the contribution of the thermal energy accompanied with the Meso → Transient Acid Meta process can be observed clearly as the rise of the signal. Fig. 6 shows the TrL signal of octopus rhodopsin and the calorimetric reference sample. The TrL signal of the reference sample shows a concave-type lens signal because the refractive index of water at this temperature decreases with increasing temperature. This is a normal thermal lens signal observed in many reports (Braslavsky and Heibel, 1992; Terazima and Hirota, 1994; Schulenberg et al., 1995). On the other hand, the TrL signal of the rhodopsin solution shows a convex lens-type signal because the dominant contribution comes from the species lens signal. The contribution of the species lens signal was subtracted by the same method as for the TG case (i.e., the contribution of the species lens signals at 24°C was determined and the lifetimes of the each step measured by transient absorption spectroscopy, and we determined the thermal lens contribution of the rhodopsin sample by subtracting the species lens contribution from the TrL signal of the rhodopsin at 24°C). The ratio of the thermal lens signal of the rhodopsin sample and that of the reference was δn_{th}(Rh*-Transient Acid Meta)/δ n_{th}(reference) = 0.98. Therefore, the enthalpy of the Transient Acid Meta was determined to be 12 ± 5 kJ/mol. The enthalpies determined for these species are summarized in Fig. 7. The activation barriers depicted in Fig. 7 were determined previously from the temperature dependence of the rate constants (Nishioku et al., 2001).

Volume change

The volume change of each photoreaction step was determined by using the PA method. Fig. 8 *A* depicts the observed PA signal of rhodopsin and BCP at 20°C. The PA

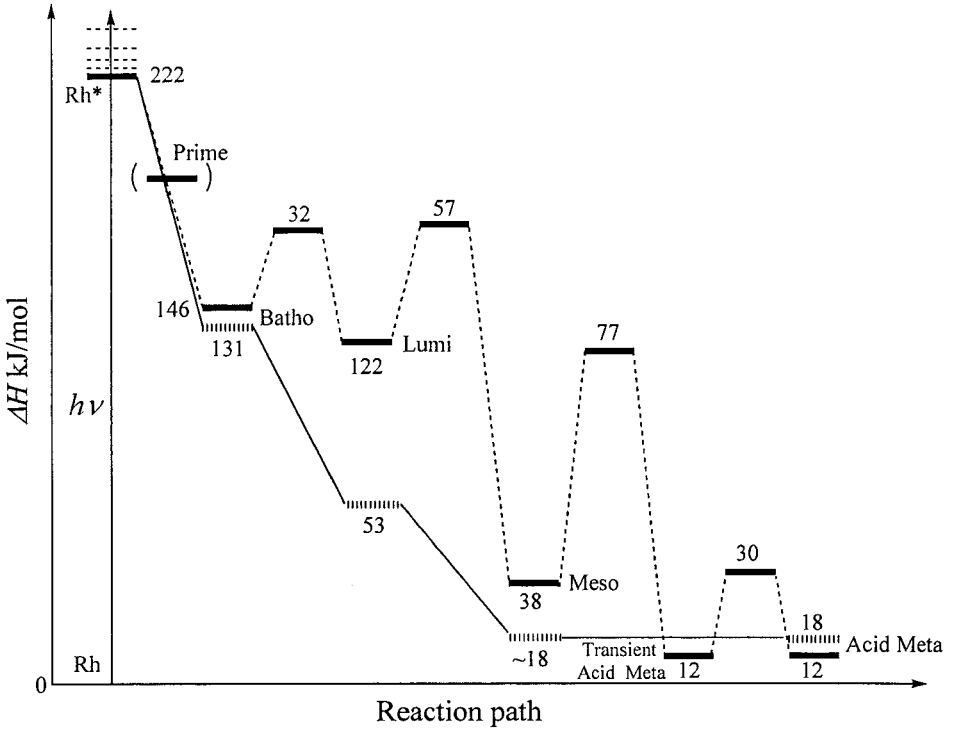

FIGURE 7 Comparison of the relative enthalpies of the various octopus photointermediates at physiological temperatures (*solid horizontal lines*) with those measured at low temperature (*dotted lines*) (Cooper et al., 1986). The activation enthalpies between these steps, measured by the temperature dependence of the reaction rates (Nishioku et al., 2001), are also shown in the figure.

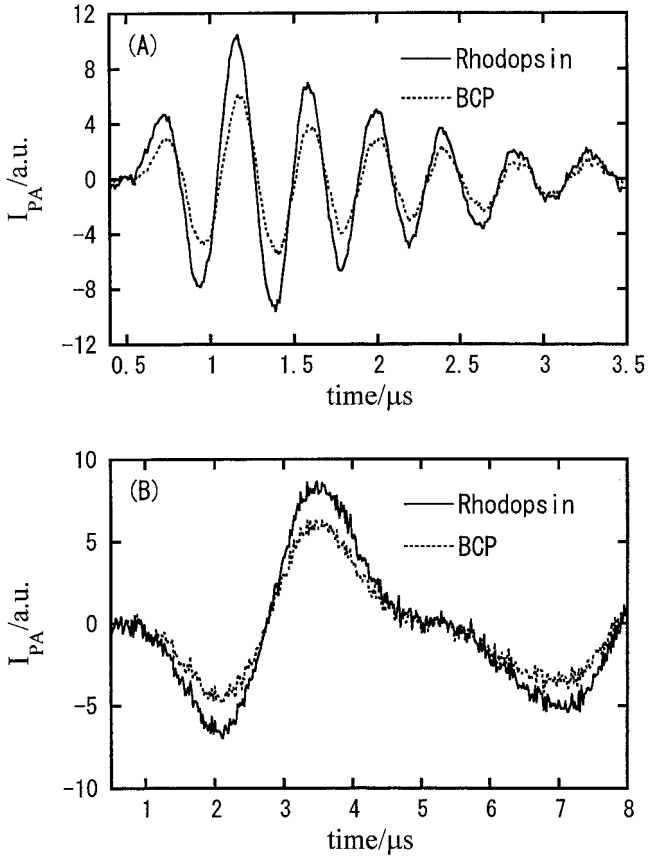

FIGURE 8 The PA signals of octopus rhodopsin sample (——) and BCP reference (· · ·) after 465-nm excitation pulse at 20°C by a fast response-piezo electro transducer (*A*) and at 35°C by a slow response-piezo electro transducer (*B*). Absorbance at 465 nm of octopus rhodopsin sample and BCP reference are the same (absorbance = 0.45, path length = 2 mm).

signal intensity represents the thermal expansion and the molecular volume changes. In this time window, the energy relaxation of Rh* (photoexcited state of rhodopsin) → Batho → Lumi → Meso and the volume change associated with Rh → Batho → Lumi → Meso are included.

The contribution of the volume change is written as (Small, 1992; Small et al., 1992; Strassburger et al., 1997)

$$P(t) = \sum_i \frac{\Psi_i^{obs}}{\tau_i} \exp(-k_i t)$$

$$\Psi_1 = \Psi_1^{obs} + \Psi_2 \frac{\tau_1}{\tau_2 - \tau_1} + \Psi_3 \frac{\tau_1^2}{(\tau_3 - \tau_1)(\tau_1 - \tau_2)}$$

$$\Psi_2 = \Psi_2^{obs} \frac{\tau_2 - \tau_1}{\tau_2} + \Psi_3 \frac{\tau_2}{\tau_3 - \tau_2} \qquad (15)$$

$$\Psi_3 = \Psi_3^{obs} \frac{(\tau_3 - \tau_1)(\tau_3 - \tau_2)}{\tau_3^2}$$

$$\Psi_i = \left(\frac{h\nu - \Phi \Delta H_i}{h\nu} + \Phi \Delta V_i \left(\frac{\rho C}{h\nu W \alpha_{th}} \right) \right)$$

where α_{th} is the thermal expansion coefficient. Ψ_i^{obs} is the apparent amplitude on the step *i* obtained by the fitting and Ψ_i is the actual amplitude and involves two contributions: thermal expansion and molecular volume change. Ψ_1, Ψ_2, and Ψ_3 represent the weight of each elementary process (subscript 1 for the production of Batho, 2 for the Batho to Lumi, and 3 for Lumi to Meso process) to the total PA signal. As the thermal energy from these steps is already obtained by the TG measurement and the rate constants of each steps are measured by transient absorption spectroscopy, the contributions of the thermal expansion and the rate constants of each steps are fixed during the curve fitting process of the PA signal. We fitted the PA signal that was measured at very low excitation laser powers (~1 μJ/pulse) the same as for the TG method to avoid the multi-photon excitation. From the relationship between Ψ_i, which was obtained by fitting and ΔV_i on Eq. 15, we obtained as $\Delta V_{Rh\text{-}Batho} = +32 \pm 3$ ml/mol, $\Delta V_{Batho\text{-}Lumi} = -5 \pm 3$ ml/mol and $\Delta V_{Lumi\text{-}Meso} = -1 \pm 1$ ml/mol.

The time constant due to the transformation of Meso→ Transient Acid Meta is much longer than the time window of the piezoelectric transducer device we used at this temperature. To obtain the volume change associated with this process, we used another piezoelectric transducer with a slower time response and measured the PA signal at higher temperature. With increasing temperature, the rate of the Meso → Transient Acid Meta process increases (4.6 μs at 35°C) and becomes comparable to the time window of the PA signal. Fig. 8 *B* shows the PA signal of rhodopsin and BCP at 35°C measured by the slower response piezo electric transducer. This signal was analyzed by the same method as above including the volume change by this process. $\Delta V_{Meso\text{-}Transient\ Acid\ Meta} = -4 \pm 3$ ml/mol was obtained. Finally, the volume change associated with the transformation of

Transient Acid Meta → Acid Meta was measured by the TG method as the volume grating component as described previously (Nishioku et al., 2001). The volume change was $\Delta V = +13 \pm 3$ ml/mol. The relative enthalpies of the octopus rhodopsin photointermediates for the ground state rhodopsin and reaction volume changes for the corresponding transition determined in this study is summarized in Table 1.

DISCUSSION

Rh* → *Batho*

Upon photoexcitation the initial event in visual pigments is the isomerization of the retinal chromophore from the 11-*cis* to the all-*trans* form. This isomerization is very fast; it occurs within 400 fs in octopus rhodopsin (Taiji et al., 1992; Kobayashi et al., 1998). The ΔH (ΔH_{Batho}) and ΔV (ΔV_{Batho}) of the Batho determined by TG and PA measurements are 146 ± 15 kJ/mol and +32 ± 3 ml/mol, respectively. Because the energy of the lowest excited state of

TABLE 1 Relative enthalpies of the octopus rhodopsin photointermediates from the ground state rhodopsin and the reaction volume changes for the corresponding transitions obtained in this study at physiological temperature

ΔH (kJ mol^{-1})					ΔV (ml mol^{-1})				
Batho	Lumi	Meso	Transient Acid Meta	Acid Meta	Rh*→Batho	Batho→Lumi	Lumi→Meso	Meso→Transient Acid Meta	Transient Acid Meta→Acid Meta
146 ± 15	122 ± 17	38 ± 8	12 ± 5	12 ± 5	+32 ± 3	−5 ± 3	−1 ± 1	−4 ± 3	+13 ± 3*

*Nishioku et al. (2001), obtained by the TG method.

bovine Rh is 222 kJ/mol (Guzzo and Pool, 1968), only 35% of this energy is released in the formation of Batho. It should be noted that this $\Delta H_{\mathrm{Batho}}$ value at physiological temperature agrees well with that determined by the cryogenically trapping method ($\Delta H_{\mathrm{Batho}}$ = 130.5 kJ/mol at −195°C (Cooper et al., 1986)). This good agreement may indicate that most of the excitation energy is stored by the distorted retinal and its interaction with the surrounding protein at both physiological temperatures and low temperatures. In other words, this correspondence suggests that the structural changes during the step of Rh to Batho are localized around the chromophore.

The energy storage mechanism is not understood well yet, but it may come from a combination of the distortion of the retinal polyene chain and the Schiff base linkage, alternation of the electrostatic interaction between the protonated Schiff base and a counterion charge, and changes of the steric interaction between the retinal and the amino acid residues in the binding pocket. Conformational changes of the retinal polyene chain and the Schiff base linkage during the Rh* to Batho step were reported using resonance Raman spectroscopy (Pande et al., 1987; Deng et al., 1991a,b; Huang et al., 1996, 1997). Furthermore, the electrostatic interaction between the protonated Schiff base and a counterion was studied by Fourier transform infrared (FTIR), which revealed that the O-H stretch frequency of a water molecule bound to the Schiff base in Batho was changed from that in Rh (Nishimura et al., 1997). (The counterion if any, for the protonated Schiff base of octopus Rh has not been identified yet (Nakagawa et al., 1999).) This change was attributed to the change of the electrostatic interaction between the protonated Schiff base and a counterion. It is very plausible that the isomerization of the retinal results in steric hindrance in the binding pocket. These strains may be the source of the high free energy of this state.

The observed volume change in the transformation of Rh* to Batho is quite large compared with those of the other subsequent processes (except the last Transient Acid Meta→ Acid Meta one). It is interesting to note that the initial steps of two other photoreceptor systems also showed a positive volume change (Rh* → Batho of bovine rhodopsin is 5 ml/mol (Gensch et al., 1998), sensory rhodopsin I is 5.5 ml/mol (Losi et al., 1999)). This change should be related to the isomerization of the retinal because, as discussed above, the structural changes in this step are rather localized around the chromophore. Since the dipole moment of retinal Schiff base does not significantly change upon isomerization, (Locknar and Peteanu, 1998) the observed volume change is not due to an electrostriction effect. Losi et al. (1999) speculated that the volume expansion reflects the partial disruption of weak interactions (e.g., hydrogen bonding) between the chromophore and the adjacent amino acid residues. Considering the structural information obtained so far, we think that the volume change could be related to the structural changes that induce the energetic stabilization, such as the distortion of the retinal and the Schiff base linkage, alteration of the electrostatic interaction, and change of steric interactions in the binding pocket.

Batho → Lumi → Meso

The ΔH of Lumi (ΔH_{Lumi}) and Meso (ΔH_{Meso}) at physiological temperatures were determined by the TG measurements to be 122 ± 17 kJ/mol and 38 ± 8 kJ/mol, respectively. The enthalpy is dramatically decreased between Lumi and Meso. Comparing these values with those determined by the cryogenic trapping method (ΔH_{Lumi} = 53.3 kJ/mol at −115°C and ΔH_{Meso} = 18 kJ/mol at −65°C (Cooper et al., 1986)), it should be noticed that ΔH_{Lumi} is very different from the value detected here. Whereas the main energy stabilization occurs between the Batho and Lumi forms at low temperature, it occurs between Lumi and Meso at physiological temperatures. Because we intuitively think that the relaxation of the molecular structure is easier at higher temperature, it is difficult to understand why the energy is more stabilized at lower temperature. This difference could mean that the conformational change depends on temperature; that is, the structure around the chromophore could be similar between the cryogenic and physiological temperatures as indicated by the absorption spectrum, but the conformation apart from the chromophore may be different. In other words, the conformational change during the Batho → Lumi process is more or less global compared with the previous transition of Rh* → Batho. On the other hand, the enthalpy of Meso is similar at both temperatures (20°C and −65°C).

From the FTIR spectra of the HOOP region at low temperatures, it was suggested that the retinal is still distorted in the Lumi and Meso forms, but the structure is

somewhat different from that in the Batho form (Nishimura et al., 1997). This different conformation may indicate that the strain of the retinal is released during this process. The O-H stretch frequency indicates that the electrostatic interaction involving the Schiff base is changed in the transformation from Batho to Lumi and Meso. These structural changes could explain the energy stabilization of Lumi and Meso from Batho. However, we should be careful because the FTIR experiments were performed at low temperature. Because the ΔH of Lumi is different at low temperature and physiological temperature, the structural change observed at low temperature could be different in solution. It is interesting to note that the ΔH_{Lumi} of octopus rhodopsin at 20°C is close to that of bovine rhodopsin at low temperature (−75°C), $\Delta H_{\mathrm{Lumi}} = 110$ kJ/mol (Cooper, 1981).

The volume changes during these processes are not significant ($\Delta V = -5 \pm 3$ ml/mol for Batho → Lumi and $\Delta V = -1 \pm 1$ ml/mol for Lumi → Meso) and are quite small considering the large energy stabilization. Probably, the energy stabilization during this process may be sensitive to the relaxation of the strain of the retinal and protein conformational change.

Meso→ Transient Acid Meta→ Acid Meta

By using the transient absorption technique, the decay of Meso was the last kinetic process detected in the photolysis of octopus Rh. However, we found a structural kinetic change leading to a new intermediate after the final change of the absorption signal, and we attributed this change to the conformation of the protein moiety far from the chromophore (Nishioku et al., 2001). This new intermediate was called Transient Acid Meta, which is transformed to Acid Meta. The enthalpy is almost completely relaxed back to the original Rh with this Transient Acid Meta form. FTIR experiments revealed that the retinal is completely relaxed at the final Acid Meta form (Nishimura et al., 1997). This relaxation could be the cause of the energy stabilization during this step. ΔH determined by the calorimetric method at 5–20°C is ~18 kJ/mol, which is the same as that of the Transient Acid Meta we obtained.

Although a small volume change was observed for Meso → Transient Acid Meta (-4 ± 3 ml/mol), a relatively large volume change was detected ($+13 \pm 3$ ml/mol) for Transient Acid Meta → Acid Meta. This observation supports the idea that the absorption change occurs first by a slight adjustment of the amino acid residues around the chromophore, and subsequently a large-scale change takes place far from the chromophore. This large volume change was speculated to be the movement of the helices. It is interesting to note that an enthalpy change was not detected during this process despite the large volume change. Therefore, entropy should drive this process.

CONCLUSION

The time-dependent values of ΔH and ΔV associated with the photolysis of octopus rhodopsin were measured at physiological temperatures by the TG, TrL, and PA methods. The enthalpy changes of Batho, Lumi, Meso, Transient Acid Meta, and Acid Meta were 146 ± 15 kJ/mol, 122 ± 17 kJ/mol, 38 ± 8 kJ/mol, 12 ± 5 kJ/mol, and 12 ± 5 kJ/mol, respectively. A large volume expansion between Rh and Batho, +32 ± 3 ml/mol, was measured. The volume changes on the subsequent reaction steps from Batho to Transient Acid Meta were rather small. Batho stores about half of the absorbed photonenergy, and this energy storage may be due to changes in the electrostatic interaction between the protonated Schiff base and a counterion and the steric hindrance of the retinal in the binding pocket induced by the isomerization. The relatively large volume change at the Rh* to Batho transition could be related to structural changes that induce the energetic stabilization, such as the conformational distortion of the retinal and the Schiff base linkage, alteration of the electrostatic interaction, and change of the protein binding pocket. The energy stabilization and volume change at subsequent steps of the photolysis can be related to the relaxation of distortion in the retinal and a change of the electrostatic interaction between the Schiff base and amino acids. Although a small volume change was observed for the Meso → Transient Acid Meta, a relatively large volume change was detected (+13 ± 3 ml/mol) during the Transient Acid Meta → Acid Meta process (Nishioku et al., 2001). This volume change suggests that the chromophore absorption change occurs first by a slight movement of the amino acid residues around the chromophore, and subsequently large changes in the protein takes place far from the chromophore. This large volume change may be responsible for the movement around the helix.

REFERENCES

Bagley, K. A., L. Eisenstein, T. G. Ebrey, and M. Tsuda. 1989. A comparative study of the infrared difference spectra for octopus and bovine rhodopsins and their bathorhodopsin photointermediates. *Biochemistry.* 28:3366–3373.

Braslavsky, S. E., and G. E. Heibel. 1992. Time-resolved photothermal and photoacoustic methods applied to photoinduced processes in solution. *Chem. Rev.* 92:1381–1410.

Cooper, A. 1979. Energy uptake in the first step of visual excitation. *Nature.* 282:531–533.

Cooper, A. 1981. Rhodopsin photoenergetics: lumirhodopsin and the complete energy profile. *FEBS Lett.* 123:324–326.

Cooper, A., S. F. Dixon, and M. Tsuda. 1986. Photoenergetics of octopus rhodopsin: convergent evolution of biological photon counters? *Eur. Biophys. J.* 13:195–201.

Deng, H., D. Manor, G. Weng, P. Rath, Y. Koutalos, T. Ebrey, R. Gebhard, J. Lugtenburg, M. Tsuda, and R. H. Callender. 1991a. A resonance Raman study of octopus bathorhodopsin with deuterium labeled retinal chromophores. *Photochem. Photobiol.* 54:1001–1007.

Deng, H., D. Manor, G. Weng, P. Rath, Y. Koutalos, T. Ebrey, R. Gebhard, J. Lugtenburg, M. Tsuda, and R. H. Callender. 1991b. Resonance Raman

study of the HOOP modes in octopus bathorhodopsin with deuterium-labeled retinal chromophores. *Biochemistry.* 30:4495–4502.

Gensch, T., J. M. Strassburger, W. Gärtner, and S. E. Braslavsky. 1998. Volume and enthalpy changes upon photoexcitation of bovine rhodopsin derived from optoacoustic studies by using an equilibrium between bathorhodopsin and blue-shifted intermediate. *Isr. J. Chem.* 38:231–236.

Guzzo, A. V., and G. L. Pool. 1968. Visual pigment fluorescence. *Science.* 159:312–314.

Hara, T., N. Hirota, and M. Terazima. 1996. New application of the transient grating method to a photochemical reaction: the enthalpy, reaction volume change, and partial molar volume measurements. *J. Phys. Chem.* 100:10194–10200.

Hashimoto, S., H. Takeuchi, M. Nakagawa, and M. Tsuda. 1996. Ultraviolet resonance Raman evidence for the absence of tyrosinate in octopus rhodopsin and the participation of Trp residues in the transformation to acid metarhodopsin. *FEBS Lett.* 398:239–242.

Huang, L., H. Deng, G. Weng, Y. Koutalos, T. Ebrey, M. Groesbeek, J. Lugtenburg, M. Tsuda, and R. H. Callender. 1996. A resonance Raman study of the C═N configurations of octopus rhodopsin, bathorhodopsin, and isorhodopsin. *Biochemistry.* 35:8504–8510.

Huang, L., H. Deng, G. Weng, Y. Koutalos, T. Ebrey, M. Groesbeek, J. Lugtenburg, M. Tsuda, and R. H. Callender. 1997. A resonance Raman study of the C═C stretch modes in bovine and octopus visual pigments with isotopically labeled retinal chromophores. *Photochem. Photobiol.* 66:747–754.

Kitagawa, T., and M. Tsuda. 1980. Resonance Raman spectra of octopus acid and alkaline metarhodopsins. *Biochim. Biophys. Acta.* 624: 211–217.

Kobayashi, T., M. Kim, M. Taiji, T. Iwasa, M. Nakagawa, and M. Tsuda. 1998. Femtosecond spectroscopy of halorhodopsin and rhodopsin in a broad spectral range of 400–1000 nm. *J. Phys. Chem. B.* 102:272–280.

Lamola, A. A., T. Yamane, and A. Zipp. 1974. Effects of detergents and high pressure upon the metarhodopsin I to metarhodopsin II equilibrium. *Biochemistry.* 13:738–745.

Locknar, S. A., and L. A. Peteanu. 1998. Investigation of the relationship between dipolar properties and *cis-trans* configuration in retinal polyenes: a comparative study using stark spectroscopy and semiempirical calculations. *J. Phys. Chem. B.* 102:4240–4246.

Losi, A., S. E. Braslavsky, W. Gartner, and J. L. S. Spudich. 1999. Time-resolved absorption and photothermal measurements with sensory rhodopsin I from *Halobacterium salinarum*. *Biophys. J.* 76:2183–2191.

Masuda, S., E. Morita, M. Tasumi, T. Iwasa, and M. Tsuda. 1993a. Infrared studies of octopus rhodopsin: existence of a long-lived intermediate and the states of the carboxylic group of Asp-81 in rhodopsin and its photoproducts. *FEBS Lett.* 317:223–227.

Masuda, S., E. Morita, M. Tasumi, T. Iwasa, and M. Tsuda. 1993b. Infrared studies of octopus rhodopsin and lumirhodopsin. *J. Mol. Struct.* 297:29–34.

Nakagawa, M., T. Iwasa, S. Kikkawa, M. Tsuda, and T. G. Ebrey. 1999. How vertebrate and invertebrate visual pigments differ in their mechanism of photoactivation. *Proc. Natl. Acad. Sci. U.S.A.* 96:6189–6192.

Nakagawa, M., S. Kikkawa, T. Iwasa, and M. Tsuda. 1997. Light-induced protein conformational changes in the photolysis of octopus rhodopsin. *Biophys. J.* 72:2320–2328.

Nakagawa, M., S. Kikkawa, K. Tominaga, N. Tsugi, and M. Tsuda. 1998. A novel photointermediate of octopus rhodopsin activates its G-protein. *FEBS Lett.* 436:259–262.

Nishimura, S., H. Kandori, M. Nakagawa, M. Tsuda, and A. Maeda. 1997. Structural dynamics of water and the peptide backbone around the Schiff base associated with the light-activated process of octopus rhodopsin. *Biochemistry.* 36:864–870.

Nishioku, Y., M. Nakagawa, M. Tsuda, and M. Terazima. 2001. A spectrally silent transformation in the photolysis of octopus rhodopsin: a protein conformational change without any accompanying change of the chromophore's absorption. *Biophys. J.* 80:2922–2927.

Ohtani, H., M. Kobayashi, M. Tsuda, and T. G. Ebrey. 1988. Primary processes in photolysis of octopus rhodopsin. *Biophys. J.* 53:17–24.

Pande, C., A. Pande, K. T. Yue, R. H. Callender, T. G. Ebrey, and M. Tsuda. 1987. Resonance Raman spectroscopy of octopus rhodopsin and its photoproducts. *Biochemistry.* 26:4941–4947.

Schulenberg, P. J., W. Gärtner, and S. E. Braslavsky. 1995. Time-resolved volume changes during the bacteriorhodopsin photocycle: a photothermal beam deflection study. *J. Phys. Chem.* 99:9617–9624.

Schulenberg, P. J., M. Rohr, W. Gärtner, and S. E. Braslavsky. 1994. Photoinduced volume changes associated with the early transformations of bacteriorhodopsin: a laser-induced optoacoustic spectroscopy study. *Biophys. J.* 66:838–843.

Small, R. J. 1992. Deconvolution analysis for pulsed-laser photoacoustics. *Methods Enzymol.* 210:505–521.

Small, R. J., L. J. Libertini, and E. W. Small. 1992. Analysis of photoacoustic waveforms using the nonlinear least squares method. *Biophys. Chem.* 42:29–48.

Strassburger, J. M., W. Gärtner, and S. E. Braslavsky. 1997. Volume and enthalpy changes after photoexcitation of bovine rhodopsin: laser-induced optoacoustic studies. *Biophys. J.* 72:2294–2303.

Taiji, M., K. Bryl, M. Nakagawa, M. Tsuda, and T. Kobayashi. 1992. Femtosecond studies of primary photoproduct in octopus rhodopsin. *Photochem. Photobiol.* 56:1003–1011.

Terazima, M. 1998. Photothermal studies of photophysical and photochemical processes by the transient grating method. *Adv. Photochem.* 24: 255–338.

Terazima, M., and T. Azumi. 1989. Limitation of absorbance measurement by using photoacoustic method. *Bull. Chem. Soc. Jpn.* 62:2862–2866.

Terazima, M., and N. Hirota. 1993. Translational diffusion of a transient radical studied by the transient grating method, pyrazinyl radical in 2-propanol. *J. Chem. Phys.* 98:6257–6262.

Terazima, M., and N. Hirota. 1994. Rise profile of the thermal lens signal: contribution of the temperature lens and the population lens. *J. Chem. Phys.* 100:2481–2486.

Tsuda, M. 1987. Photoreaction and phototransduction in invertebrate photoreceptors. *Photochem. Photobiol.* 45:915–931.

Tsuda, M. 1979. Transient spectra of intermediates in the photolytic sequence of octopus rhodopsin. *Biochim. Biophys. Acta.* 545:537–546.

Tsuda, M., and T. G. Ebrey. 1980. Effect of high pressure on the absorption spectrum and isomeric composition of bacteriorhodopsin. *Biophys. J.* 30:149–157.

Tsuda, M., T. Tsuda, Y. Terayama, Y. Fukada, T. Akino, G. Yamanaka, L. Stryer, T. Katada, M. Ui, and T. G. Ebrey. 1986. Kinship of cephalopod photoreceptor G-protein with vertebrate transducin. *FEBS Lett.* 198: 5–10.

van Brederode, M. E., T. Gensch, W. D. Hoff, K. J. Hellingwerf, and S. E. Braslavsky. 1995. Photoinduced volume change and energy storage associated with the early transformations of the photoactive yellow protein from *Ectothiorhodospira halophila*. *Biophys. J.* 68:1101–1109.

Zhang, D., and D. Mauzerall. 1996. Volume and enthalpy changes in the early steps of bacteriorhodopsin photocycle studied by time-resolved photoacoustics. *Biophys. J.* 71:381–388.